



## Evaluation of some supports to RuSn catalysts applied to dimethyl adipate hydrogenation

J. Fontana<sup>a</sup>, C. Vignado<sup>a</sup>, E. Jordao<sup>a</sup>, F.C.A. Figueiredo<sup>b,1</sup>, W.A. Carvalho<sup>b,\*</sup>

<sup>a</sup> Laboratory of Catalytic Processes Development, Chemical Systems Engineering Department, Faculty of Chemical Engineering, Universidade Estadual de Campinas, Cidade Universitária Zeferino Vaz, CP. 6066, CEP 13083-970, Campinas, SP, Brazil

<sup>b</sup> Centro de Ciências Naturais e Humanas, Universidade Federal do ABC, Rua Santa Adélia, 166, Santo André-SP, CEP 09210-170, Brazil

### ARTICLE INFO

#### Article history:

Received 10 November 2010

Received in revised form 4 February 2011

Accepted 14 February 2011

Available online 30 March 2011

#### Keywords:

Hydrogenation  
Ruthenium  
Diol  
Bimetallic catalyst  
SMSI

### ABSTRACT

The present work evaluates different supports, La<sub>2</sub>O<sub>3</sub>, TiO<sub>2</sub>-R, TiO<sub>2</sub>-A, SiO<sub>2</sub>, Nb<sub>2</sub>O<sub>5</sub> and aluminum pillared clays (Al-PILC), in the preparation of bimetallic RuSn catalysts. The catalysts were prepared by impregnation method, calcined and reduced at 673 K and characterized by temperature programmed reduction (TPR). Dimethyl adipate hydrogenation reactions were carried out at 50 bar and 528 K in liquid phase. The presence of reducible support species showed a promoting effect over both activity and selectivity to 1,6-hexanediol, suggesting a combined effect between the support and the promoter (tin). Active sites obtained in RuSn/TiO<sub>2</sub>-anatase, RuSn/SiO<sub>2</sub> and RuSn/Nb<sub>2</sub>O<sub>5</sub> catalysts were suitable for the hydrogenation of the ester group of dimethyl adipate, leading 1,6-hexanediol formation. Both catalytic tests and TPR analysis show the great support influence on the formation of active phase, as well as on the reducibility of the metallic species, which was attributed to different interaction among metals and the solid support.

© 2011 Elsevier B.V. All rights reserved.

### 1. Introduction

Several attempts have been made to develop new specific catalytic systems with suitable activity and selectivity to a large variety of products from fine chemistry. The catalytic hydrogenation of dicarboxylic esters as dimethyl adipate (DMA), a C6 linear dicarboxylic ester, provides a wide variety of valuable products with great industrial relevance while they are used as raw material in a variety of chemicals, pharmaceuticals and biodegradable polymers. Among the main products obtained in dimethyl adipate hydrogenation, it is possible to produce 1,6-hexanediol, monoesters, cyclic ethers, lactones, alcohols and hydrocarbons.

The industrial interesting on diols is focused on their use as intermediary products to the production of polyesters, polyurethanes, surface coatings and adhesives. Specifically, the 1,6-hexanediol is a valuable intermediary for the synthesis of di-substituted products due its structural configuration containing two hydroxyl terminal groups in a linear chain [1]. Both  $\epsilon$ -caprolactone ( $\epsilon$ -CPL) and adipic acid monomethyl ester (MME) are widely used as raw materials to polyesters thermoplastics and lubricants and polymeric plasticizers, respectively. The  $\gamma$ -

caprolactone ( $\gamma$ -CPL) is used as flavor additive in foods and tobaccos and as raw material for insecticides. Methyl caproate is used as flavor and fragrance component [2].

The catalytic hydrogenation of carbonyl groups is usually carried out over Os, Ir, Pt, Rh, Ru (Group VIII metal) and also over Ni, Cu and Co, due their ability in hydrogenation reactions [3]. However, they require drastic operational conditions as high pressures and temperatures reactions [4]. In previous studies, we observed that ruthenium catalysts have showed high activities in the hydrogenation of dimethyl adipate, while Pd, Pt and Rh produced larger quantities of undesirable products [5,6]. Monometallic ruthenium systems are not suitable to produce diol with a high selectivity. On the other hand, bimetallic ruthenium catalysts lead the reaction mainly towards diol. The addition of a second metal enhances the selectivity results, especially tin [7]. It was verified that the presence of Lewis acid sites, obtained from tin species (Sn<sup>n+</sup>) in ruthenium bimetallic catalyst, contributes to the polarization of C=O bond, increasing diol selectivity.

The supports also have been successfully used to improve some catalytic properties. Reducible oxides have been extensively studied once they can present the SMSI effect (strong metal-support interaction), characterized by the formation of reducible oxide species when submitted to high reduction temperature [8,9].

The use of aluminum pillared clay becomes interesting once it presents great thermal stability and the possibility of change its properties, as acidity and porosity. Due to the small size of its par-

\* Corresponding author. Tel.: +55 11 4996 0174; fax: +55 11 4996 0174.

E-mail address: [wagner.carvalho@ufabc.edu.br](mailto:wagner.carvalho@ufabc.edu.br) (W.A. Carvalho).

<sup>1</sup> Tel.: +55 11 4996 0174; fax: +55 11 4996 0174.

ticles ( $<2\ \mu\text{m}$ ) and to the high intercalation capacity, some clay minerals present high surface area, and the interlayer space can improve the catalyst's selectivity [10]. Moreover, the clay's pillarization contributes to increase the acidity of the material, which should affect both the activity and selectivity of the catalysts [2].

The effectiveness of the supported catalysts depends on the preparation method, including the reduction and calcination process. Conventional impregnation and incipient wetness technique are the methods most frequently reported for the preparation of supported ruthenium catalyst [11]. It was found in a previous work involving RuSn catalyst that a nominal metal loading, respectively 2 wt% and 4.7 wt% for ruthenium and tin, is the most appropriated Ru:Sn ratio to dimethyl adipate hydrogenation [12].

In this work, it was reported the support effect in the hydrogenation of DMA on bimetallic ruthenium-tin based catalyst systems in order to obtain 1,6-hexanediol. The supports tested were  $\text{La}_2\text{O}_3$ ,  $\text{TiO}_2$  and  $\text{Nb}_2\text{O}_5$ , known as reducible oxides, and the non-reducible  $\text{SiO}_2$  and aluminum pillared clays. The catalysts were obtained by the impregnation method and characterized by temperature programmed reduction analysis (TPR). The combined effect of tin and support species on 1,6-hexanediol production and the influence of different chemical nature of the support on the formation of the active sites were investigated.

## 2. Experimental

The catalysts were prepared by the impregnation method in aqueous suspension (excess solvent), in order to obtain catalysts with nominal content of 2 wt% and 4.7 wt% of Ru and Sn, respectively, corresponding to an atomic ratio Sn:Ru equal to 2. The supports used were lanthanum oxide– $\text{La}_2\text{O}_3$  (Aldrich), titanium oxide– $\text{TiO}_2$ –rutile (Synth), titanium oxide– $\text{TiO}_2$ –anatase (Aldrich), silicon dioxide– $\text{SiO}_2$  (Alfa), niobium oxide– $\text{Nb}_2\text{O}_5$  (Aldrich) and montmorillonite aluminum pillared clay–Al-PILC (Fluka), which were crushed and sieved to fractions smaller than 0.045 mm. The precursor salts of the metals were  $\text{RuCl}_3\cdot\text{H}_2\text{O}$  (Aldrich, 98%) and  $\text{SnCl}_4\cdot 2\text{H}_2\text{O}$  (Aldrich, 98%). The impregnation was accomplished through the addition of support and the solution containing the metallic precursors in a flask kept in a route vacuum evaporator with bath at 333 K for 5 h to remove the excess solvent. Next, the material was kept in an oven for 12 h at a temperature of 393 K for complete drying of the solid. RuSn/ $\text{Al}_2\text{O}_3$  data obtained in previous work [7] were used as comparison results. Monometallic catalysts of ruthenium and tin were prepared in a similar way, except by the addition of only one metal to the support.

The catalysts were calcined at 673 K with a heating rate of  $10\ \text{K min}^{-1}$  under synthetic air flow of  $50\ \text{mL min}^{-1}$  for 4 h. After calcination, the catalysts were submitted to a reduction process under hydrogen flow of  $40\ \text{mL min}^{-1}$  at 673 K for 2 h, and a heating rate of  $10\ \text{K min}^{-1}$ . Such parameters, calcination and reduction, were determined and found to be effective in previous work [13].

The catalyst supported on Al-PILC was submitted to treatment with barium to reduce the acidity (RuSn/Al-PILC–Ba). Each 2 g of catalyst was added to 200 mL of a solution of  $\text{Ba}(\text{NO}_3)_2$   $0.1\ \text{mol L}^{-1}$  and kept under magnetic stirring at room temperature for 2 h. Solid phase was separated by vacuum filtration and washed with deionized water until absence of barium cations in the aqueous phase. The solid was oven dried at 383 K for 6 h and subjected to calcination and reduction treatments in the similar way than those described above.

The hydrogenation of dimethyl adipate was performed in a Parr high pressure reactor, equipped with a mechanical stirring shaft with adjustable speed and a gas supply system. The reactions were conducted in a liquid medium, using 1,4-dioxane as solvent and tetradecane as internal standard at 528 K and 50 bar

$\text{H}_2$ , under constant stirring of 1500 rpm. Before the start of the reaction, the system was kept for 1 h under the reaction conditions for the re-activation of the catalyst. The reaction starts by adding 7 g of substrate (DMA) and 1.8 g of tetradecane to the reactor containing 1.4 g of catalyst. Samples were taken every hour until it was completed 15 h of reaction. The stirring speed was considered to be sufficient to keep the system free of diffusion limitations.

The reaction products were separated and quantified by gas chromatography through a HP-6890 equipment, using a Carbowax capillary column (30 m, 0.25 mm internal diameter and 0.25 mm film thickness) and flame ionization detector (FID).

The analysis of temperature programmed reduction (TPR) were carried out using a Quantachrome model Chembet-3000 device, coupled to a quartz reactor under a flow of  $80\ \text{mL min}^{-1}$  of a reductive mixture of 95%  $\text{N}_2$  and 5%  $\text{H}_2$ . Analysis temperature was programmed to vary from 298 to 1273 K, with  $10\ \text{K min}^{-1}$  heating rate.

## 3. Results and discussion

### 3.1. TPR analysis

In order to evaluate the interactions between the metal-promoter and metal-support interactions and the reduction behavior of all the catalysts species, temperature programmed reduction analysis were carried out before catalysts reduction. The analyses give information about the active phases in the different systems studied and the effects of the nature of the support in the reduction of ruthenium and tin.

The TPR profile obtained from monometallic (Ru) and bimetallic (RuSn) systems are compared in Figs. 1 and 2, respectively, where the hydrogen consumption peak is a consequence of reduction event on the metallic particles or on the support. The results related to the catalysts supported on Al-PILC are presented in Fig. 3.

It is noticed that the reduction profiles are quite distinct from one another, especially among the bimetallic catalysts, making clear the influence of the support on the reducibility of the metals. This behavior could be related to the different metal-support interactions established. It is assumed that, the higher the reduction temperature of the components in the catalyst, the greater the interaction between metal and support.

Except the systems supported on niobia and lantania which presented reductions peaks assigned to the support reduction, and on rutile phase titania that presented two ruthenium reduction peaks,

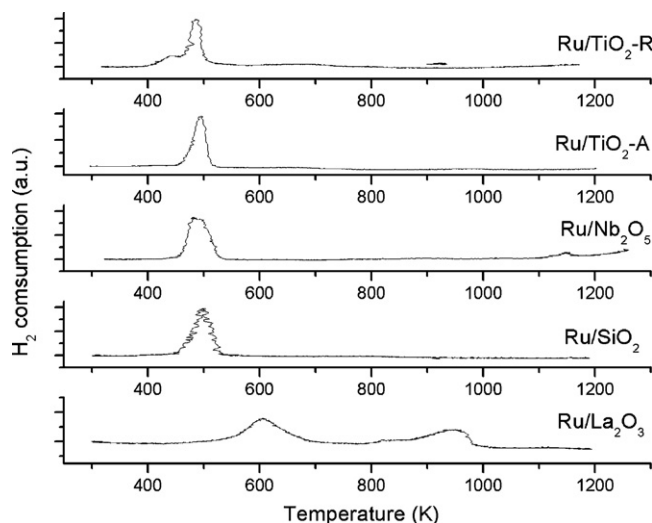


Fig. 1. TPR of monometallic Ru systems over different supports.

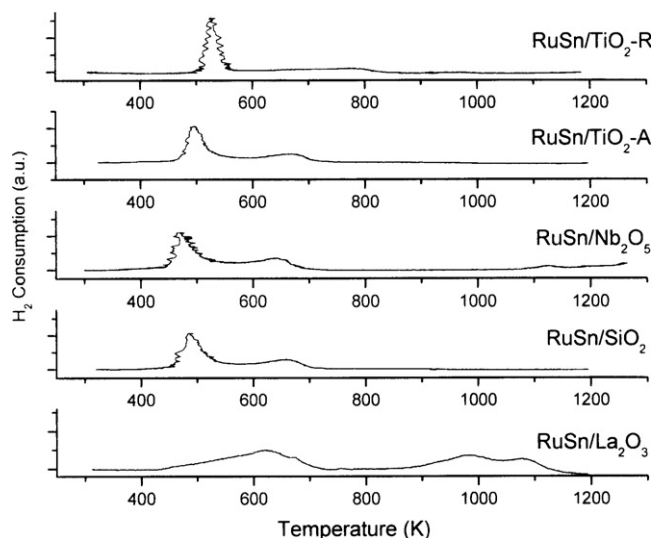


Fig. 2. TPR of bimetallic RuSn systems over different supports.

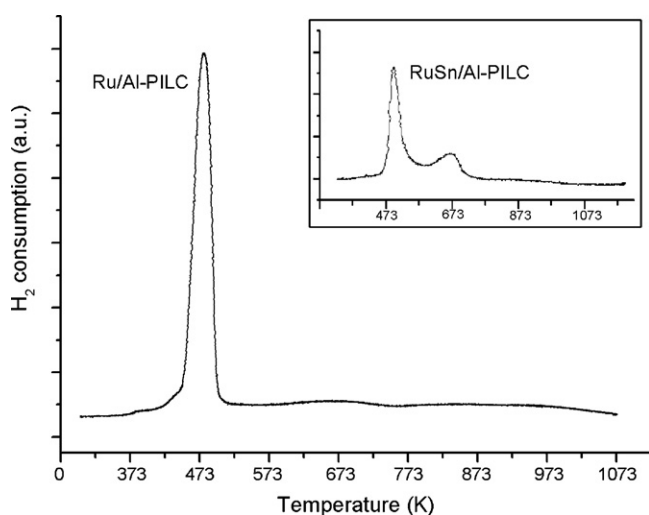


Fig. 3. TPR of RuSn/Al-PILC systems over different supports.

all the other monometallic systems showed only one reduction peak related to ruthenium.

Ru/TiO<sub>2</sub>-R shows, besides the main peak at 480 K, a shoulder at 440 K, probably related to the ruthenium species interacting less vigorously with the support [14]. Comparing the profiles of reduced catalysts supported on TiO<sub>2</sub>-A, SiO<sub>2</sub>, Nb<sub>2</sub>O<sub>5</sub> (Fig. 1) and Al-PILC (Fig. 3), the reduction temperature of ruthenium is around 480 K and 490 K, corresponding to the reduction of RuO<sub>2</sub> oxide species (Ru<sup>4+</sup> to Ru<sup>0</sup>) formed during the calcination step [15]. However, for lanthia supported catalyst the ruthenium reduction was observed at 600 K and 620 K for mono and bimetallic catalysts (Table 1), respectively. The hydrogen consumption peak at 1023 K is attributed to the support reduction. The reduction of tin supported on monometallic Sn/La<sub>2</sub>O<sub>3</sub> occurs at 1080 K, referring to the reduction of tin oxide (SnO<sub>2</sub>) formed after calcination step. This temperature is the highest observed among the monometallic tin catalysts (Table 1). These results indicate a strong interaction between the metals and the lanthia, which makes it more difficult both the reduction and the interaction between the metals. Furthermore, the reduction profiles of the bimetallic catalyst RuSn/La<sub>2</sub>O<sub>3</sub> is very close to the sum of the profiles obtained to monometallic Ru/La<sub>2</sub>O<sub>3</sub> and Sn/La<sub>2</sub>O<sub>3</sub> catalysts. This behavior shows that there

**Table 1**  
Reduction peak temperature of monometallic systems.

Support	Monometallic catalysts Reduction peak (K)		Bimetallic catalysts Reduction peak (K)	
	Ru	Sn	Ru	Sn
TiO <sub>2</sub> -R	440/480	900	530	530
TiO <sub>2</sub> -A	490	870	490	660
Nb <sub>2</sub> O <sub>5</sub>	490	920	470	640
SiO <sub>2</sub>	490	920	490	650
La <sub>2</sub> O <sub>3</sub>	600	1080	600	980
Al-PILC	480	900	490	670

was little interaction between the metals, probably caused by the strong interaction between each metal in particular and the support as discussed above.

The catalytic tests presented below show that the catalyst RuSn/La<sub>2</sub>O<sub>3</sub> had low conversion and selectivity values. This is justified by the possible blocking of the active metal (decoration effect), caused by partially reduced species of the support (LaO<sub>x</sub>). This effect could also occur due to the presence of not reduced tin species. Tin could have stood in the oxide form even after reduction treatment at 673 K, not contributing to the carbonyl activation.

The decoration effect is commonly found in catalysts supported on reducible oxides, including TiO<sub>2</sub>, Nb<sub>2</sub>O<sub>5</sub> and La<sub>2</sub>O<sub>3</sub> after undergoing high temperature reduction, especially in the presence of VIII group metals [16–18]. Under this condition, reduced oxide species would partially cover metal particles in the active sites. On the other hand, the formation of species such as reduced TiO<sub>x</sub> would be responsible by the polarization of carbonyl groups and thus contributing to the increase in activity and selectivity. Previous results show that these species are essential for the selectivity to diol, inhibiting excessive hydrogenation of the reactant molecules [11].

All the bimetallic RuSn systems (Figs. 2 and 3) presented a slight difference on ruthenium reduction temperature compared to the monometallic systems (Fig. 1). Some authors [19,20] attribute such behavior to an increase on ruthenium dispersion in the presence of tin.

Opposite to the behavior observed in La<sub>2</sub>O<sub>3</sub> supported catalysts, all the other systems showed metal reduction profiles for bimetallic catalysts quite different from the monometallic reduction profiles. RuSn/TiO<sub>2</sub>-R catalyst shows only one peak of hydrogen consumption, with small shift to higher temperature on the reduction of

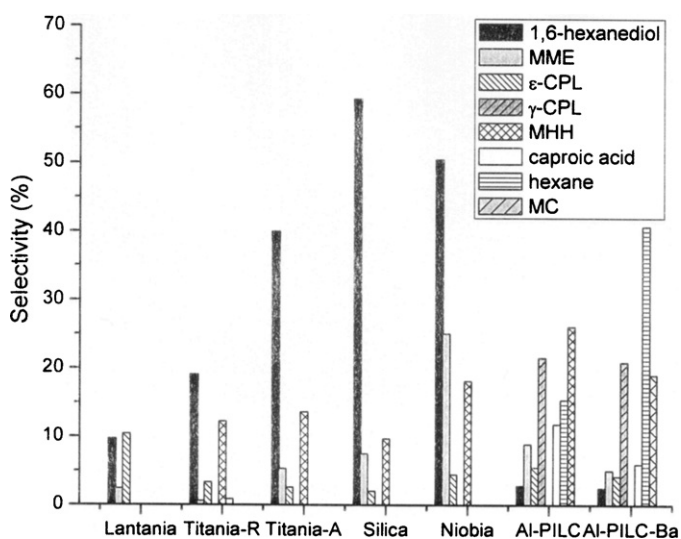


Fig. 4. Selectivity of some relevant products formed over the supported RuSn catalysts after 15 h reaction time.

active metal in monometallic sample. This result may represent effective interaction between ruthenium and tin, which are closely interacting, probably in the form of an alloy. Regarding to the results of the catalytic tests, this new phase was fairly active, but presented low diol selectivity (Table 2). Such behavior can be explained by the fact that rutile phase titanium oxide is thermodynamically and structurally more stable than anatase phase and it is not easily reduced ( $\text{Ti}^{4+}$  to  $\text{Ti}^{3+}$ ). The  $\text{Ti}^{3+}$  ions fixed in the surface lattice of anatase titania are easier to diffuse to the surface of ruthenium than on rutile surface, and metal–support interaction becomes easier [21,22]. Thus, metal–support interactions over titania anatase phase are greater than those expected for the rutile one.

Reduction profiles obtained to RuSn supported over  $\text{TiO}_2$ -A,  $\text{SiO}_2$ ,  $\text{Nb}_2\text{O}_5$  and Al-PILC are quite similar. In all cases the reduction peak of tin in the bimetallic catalysts is shifted to a lower temperature compared to monometallic tin catalysts. This behavior reveals that the interaction between tin and these supports is less intense than in  $\text{La}_2\text{O}_3$ , which allows greater interaction with the active metal. So it becomes easier the reduction of tin for hydrogen spillover from the active metal. Thus, the reduction of tin is influenced by the nature of support.

The accepted model to explain the promoter effect of tin at C=O hydrogenation is based on the formation and stabilization of ionic species of tin near to the active metal [3]. As Lewis acid sites, the ionic tin species interact with the carbonyl oxygen promoting the reaction by increasing the polarity of the ester group, which leads to the 1,6-hexanediol formation. Another explanation is the presence of partially reduced support species formed after reduction at high temperature (e.g.:  $\text{LaO}_x$ ,  $\text{NbO}_x$ ,  $\text{TiO}_x$ ) that, as well as the ionic tin, act on the polarization of C=O ester bond.

The TPR of lantania and niobia supported systems shows reduction peaks of the support after 1073 K. The oxide supports reductions could also have occurred concomitantly with the reduction of metals in the presence of ruthenium by hydrogen spillover that could have caused metal sites blocking, directly influencing the catalyst activity.

### 3.2. Catalytic tests

Different materials with different characteristics were used as a support. The main products formed after 15 h have and their concentrations are presented in Table 2. In order to compare the behavior, it was included data from the monometallic ruthenium catalysts.

Typically, the bimetallic catalysts were more active than the respective monometallic ones, except to lantania supported catalysts.

There is a strong dependence on the conversion of the substrate according to the support on which the active phase is dispersed. Among the oxide supported catalysts, RuSn/ $\text{TiO}_2$ -R, RuSn/ $\text{TiO}_2$ -A, RuSn/ $\text{SiO}_2$  and RuSn/ $\text{Al}_2\text{O}_3$  [7] showed the higher conversions, 51.5%, 52.9%, 90% and 56.6%, respectively. RuSn/ $\text{Nb}_2\text{O}_5$  presented 31.0% dimethyl adipate conversion under the same conditions, while on RuSn/ $\text{La}_2\text{O}_3$  system the conversion was only 11.0%. In the absence of catalyst the conversion was 3.6%. The use of pillared clay as support makes the system more active, reaching almost total dimethyl adipate conversion after 15 h reaction time and more than 50% conversion in less than 2 h reaction time.

The different conversion values may be related to the chemical nature of the support acting directly in the formation of active sites on metal–support interface, also verified on TPR analysis. It is also significant the characteristics of the supports as the SMSI effect. It affects the catalytic activity according to the geometric effect, due to the surface decoration of the active metal by partial reduced species of the support, but also by a promoting action of such species in close contact with the active metal. This creates a polarity that favor the interaction of the oxygen atom of the C=O bond with the catalyst surface, involving hydrogen migration from the metallic atoms to molecules adsorbed on the catalyst's surface. It was noticed that the catalysts supported on oxides with stronger SMSI effects,  $\text{La}_2\text{O}_3$  and  $\text{Nb}_2\text{O}_5$ , showed the lowest activities. Since the catalysts supported on  $\text{TiO}_2$  rutile phase, characterized by a SMSI effect less intense, and  $\text{SiO}_2$ , a non-reducible oxide, the activities were higher. In  $\text{TiO}_2$  anatase phase, although the SMSI effect is greater than the rutile, the results suggest that the species of partially reduced support have more intensive promoter function on the reaction.

At presence of tin, despite higher activities, the selectivity to diol and the products distribution were affected as well. Thus, the presence of promoted tin is essential to 1,6-hexanediol formation at worthy quantities. Moreover, monometallic catalysts revealed to be able to the cleavage of the O–CH<sub>3</sub> bond in the ester group giving the adipic acid monomethyl ester (MME), in agreement to previous results [11]. However, the trend over bimetallic catalysts is the suppression on monomethyl ester formation.

The selectivities of the main products obtained in the dimethyl adipate hydrogenation after 15 h of reaction over the bimetallic catalysts tested are compared in Fig. 4.

**Table 2**  
Concentration of hydrogenation products from dimethyl adipate reaction catalyzed by monometallic and bimetallic catalysts supported on different solids (after 15 h reaction time).

Catalyst	Conv. (%)	Concentration (mmol L <sup>-1</sup> )									
		ane	ol	$\epsilon$ -ona	oic	diol	$\gamma$ -ona	HMH	MC	MME	Other
Blank	3.6	2.0	–	–	–	–	–	–	4.7	2.2	4.7
Ru/Al-PILC	97.0	24.1	3.5	11.0	–	3.0	–	–	11.2	40.0	294.2
RuSn/Al-PILC	98.4	42.0	–	15.0	32.2	7.6	58.9	–	71.3	24.3	140.3
Ru/Al-PILC Ba	93.8	34.9	–	18.1	–	16.0	–	–	10.3	102.7	202.5
Ru-Sn/Al-PILC Ba	98.9	145.1	6.2	14.9	21.4	8.8	74.5	–	67.7	17.9	37.5
Ru/ $\text{TiO}_2$ - A	17.1	–	–	2.1	–	2.0	–	3.8	–	40.9	51.2
RuSn/ $\text{TiO}_2$ - A	52.9	–	–	5.5	–	85.4	–	29.0	–	11.4	82.4
Ru/ $\text{TiO}_2$ - R	16.7	–	–	5.4	1.9	3.8	–	9.07	–	18.2	32.0
RuSn/ $\text{TiO}_2$ - R	51.5	–	2.2	6.4	1.7	51.7	–	26.9	–	1.8	154.8
Ru/ $\text{SiO}_2$	6.2	1.5	–	1.4	1.3	2.1	–	6.3	–	16.5	–
RuSn/ $\text{SiO}_2$	56.6	–	0.6	4.6	–	135.8	–	22.1	–	17.2	51.5
Ru/ $\text{Nb}_2\text{O}_5$	15.5	–	–	–	–	8.8	–	14.7	–	7.9	28.6
RuSn/ $\text{Nb}_2\text{O}_5$	31.0	–	–	5.0	–	63.0	–	19.9	–	30.7	6.5
Ru/ $\text{La}_2\text{O}_3$	52.4	4.4	–	–	–	2.3	–	–	–	59.1	146.1
RuSn/ $\text{La}_2\text{O}_3$	8.9	–	0.7	4.3	–	4.0	–	–	–	0.9	31.3

ane: hexane; ol: hexanol;  $\epsilon$ -ona:  $\epsilon$ -caprolactone; oic: caproic acid; diol: 1,6-hexanediol;  $\gamma$ -ona:  $\gamma$ -caprolactone; MHM: methyl 6-hydroxyhexanoate; MC: methyl caproate; MME: adipic acid monomethyl ester; other: not identified products.

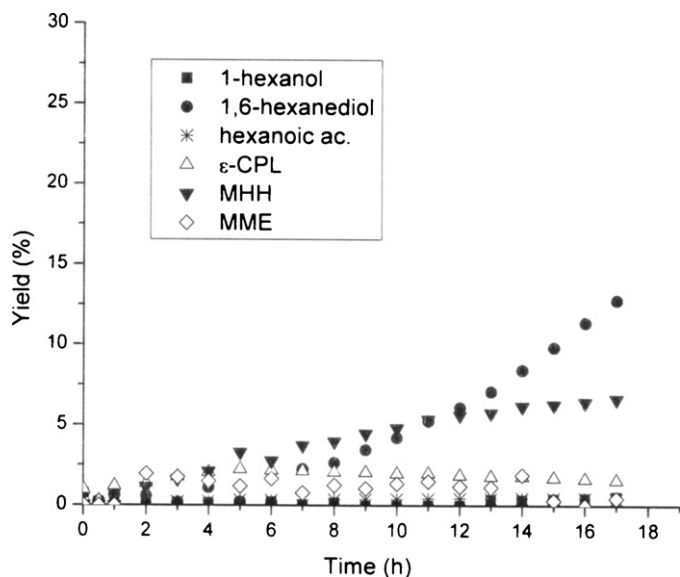


Fig. 5. Yield of dimethyl adipate hydrogenation by RuSn/TiO<sub>2</sub>-R catalyst.

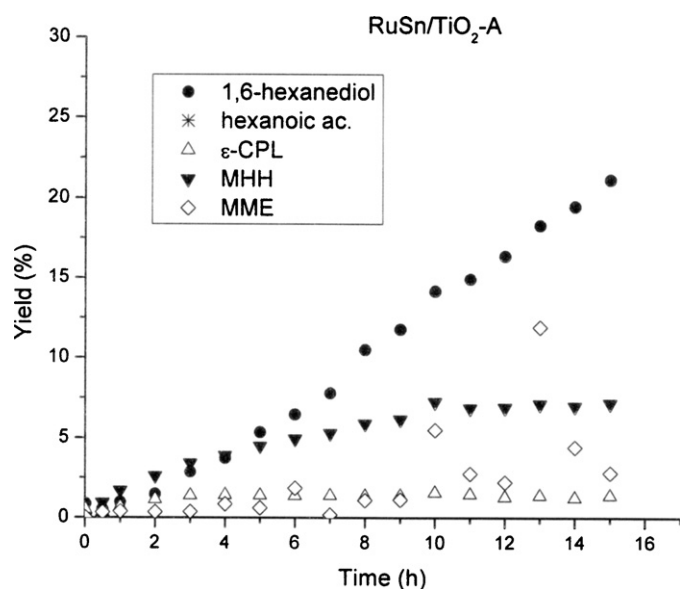


Fig. 6. Yield of dimethyl adipate hydrogenation by RuSn/TiO<sub>2</sub>-A catalyst.

The differences in the selectivities emphasize changes in the active metallic sites on the catalyst surface, especially regarding to 1,6-hexanediol formation, which appears to be related to an intrinsic role of the support.

The yields of bimetallic RuSn systems supported on TiO<sub>2</sub>-R and TiO<sub>2</sub>-A are displayed in Figs. 5 and 6. The main products obtained by RuSn/TiO<sub>2</sub>-R catalyst were MHH and 1,6-hexanediol. RuSn/TiO<sub>2</sub>-R catalyzed system shows a continuous increase in the yield of 1,6-hexanediol reaching 12.8% after 15 h reaction time. In this case it was observed that the formation of diol became significant from 7 h reaction time until the end. This suggests that diol formation includes an induction period necessary to obtain the selective catalytic sites. In this system we can also observe that the concentration of the adipic acid monomethyl ester decreases with the time to be fully converted. It is also observed formation of MHH, hexanoic acid and  $\epsilon$ -caprolactone.

The reaction catalyzed by RuSn/TiO<sub>2</sub>-A did not lead to the formation of hexane and hexanoic acid, unlike those systems that

had the rutile phase as a support. The reaction provided only 1,6-hexanediol, MHH,  $\epsilon$ -caprolactone and adipic acid monomethyl ester. These catalysts showed high selectivity to diol (23.8% yield), higher than the results found when the support was rutile. For the catalyst RuSn/TiO<sub>2</sub>-A, the production of MHH and  $\epsilon$ -caprolactone were similar to that catalyzed by RuSn/TiO<sub>2</sub>-R.

The main difference between the systems supported on rutile and anatase is the consumption of the adipic acid monomethyl ester which is higher when the catalyst is supported on anatase. Moreover, we observe that over RuSn/TiO<sub>2</sub>-A the amount of diol formed is higher, accomplished to a greater consumption of monomethyl ester.

As discussed above, when rutile phase titania is used, the metal–support interaction is weaker than that observed with anatase phase titania. It is suggested that in the absence of the SMSI effect, the stability of reduced Ti<sup>3+</sup> species in contact with the active metal is low. Therefore these species can be easily oxidized to Ti<sup>4+</sup>. The presence of partially reduced species as Ti<sup>3+</sup> is considered as one reason of the reaction selectivity, since new sites could be created by the metal–support (ruthenium–titanium) interaction. Therefore, the use of rutile phase titania becomes less appropriate than anatase.

Positively charged tin species act as electron receptors, favoring the adsorption of reactant molecules on the catalyst surface, since these molecules interact with the catalyst surface through the oxygen atoms. Thus, the bonding strength between metals and oxygen reflects on the catalytic properties. The strength of this interaction can be explained by the values of heat of formation. The value related to SnO<sub>2</sub> (−239.3 kJ mol<sup>−1</sup>) is greater than that of RuO<sub>2</sub> (−285.8 kJ mol<sup>−1</sup>), so the affinity of tin to oxygen will be greater than ruthenium [23].

In this study, the possible metal–support interaction may have been sufficient to create catalytic sites, but not strong enough to inhibit the adsorption of hydrogen on the active metal particles. It must be observed that the catalytic activity of these catalysts is higher than those values obtained with the catalysts supported on rutile. It seems that the greater the amount of Lewis acid sites, the higher the conversion of DMA and selectivity to diol. For systems with a reduced number of active sites, adsorption is difficult, which inhibits the hydrogenation of DMA and the production of EMM. Furthermore, several studies have confirmed that isolated metal sites have low activity in the hydrogenation of carbonyl groups, which is due to the weak adsorption of the metal carbonyl [7,11,24].

Considering the present data and those obtained by other authors, we can suppose that the increase on selectivity and activity of bimetallic catalysts is related to the joint award of several factors such as changes in particle size of the active metal [25–28], nature of the crystalline phase [19] and the Lewis acid sites (according to the oxidation state of the promoters and the presence of reduced species from the support).

The system catalyzed by RuSn/La<sub>2</sub>O<sub>3</sub> showed  $\epsilon$ -caprolactone, MHH and 1,6-hexanediol as main products (Fig. 7).

Considering the basicity of lantania, the formation of  $\epsilon$ -caprolactone can be attributed exclusively to dimethyl adipate hydrogenation followed by intramolecular nucleophilic addition through HHM intermediary product. Furthermore, it is not possible to identify a real correlation between the lactone formation and the data obtained for the other catalysts. The 1-hexanol can be originated from the dimethyl adipate. The 1,6-hexanediol could be related to intermediary products hydrogenation. However, kinetic results of RuSn/La<sub>2</sub>O<sub>3</sub> system did not indicate any intermediary products consumption, so the formation of diol can be associated to direct hydrogenation of reactant molecule (Fig. 8).

The kinetic monitoring system RuSn/SiO<sub>2</sub>, shown in Fig. 9, reveals that the catalyst presents high activity and selectivity to 1,6-hexanediol.

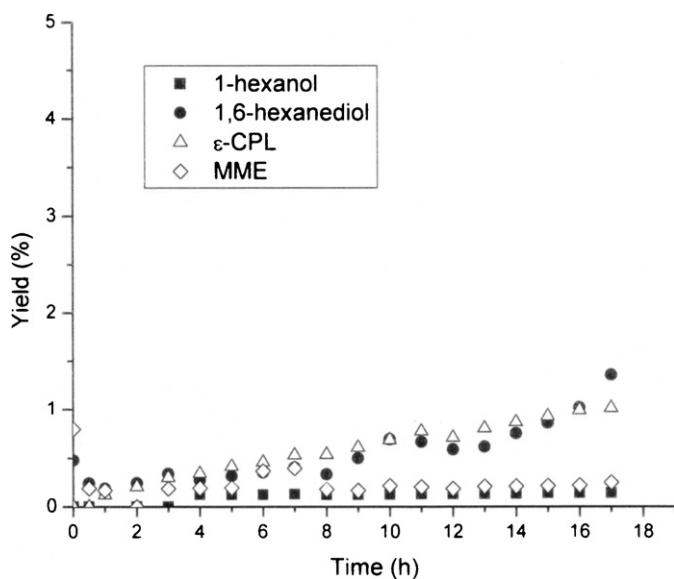


Fig. 7. Yield of dimethyl adipate hydrogenation by RuSn/La<sub>2</sub>O<sub>3</sub> catalyst.

As already mentioned, silica is not a partially reducible oxide, even in the presence of ruthenium. Therefore silica is not subject to the formation of species that would block some active sites that avoid excessive hydrogenation reagent. However, despite the high activity of RuSn/SiO<sub>2</sub> system, the reaction selectivity was also quite satisfactory. The concentration of 1,6-hexanediol reached a yield 33.6% and selectivity around 60% after 15 h reaction time, without reaching the equilibrium. Products as 1-hexanol, ε-caprolactone, MHH and adipic acid monomethyl ester were formed in small quantities.

The yields obtained for RuSn/Nb<sub>2</sub>O<sub>5</sub> catalyst along 15 h reaction time are presented in Fig. 10. Instead of being a reducible oxide, niobia showed satisfactory results both on the reaction activity and selectivity to 1,6-hexanediol. The production of diol constantly increased during the reaction, reaching selectivity values as high as 50%. A particular feature of this system was the lowest formation of “other” products (9.6%), when compared to the other catalysts tested. The ε-caprolactone was also formed, but in relatively low concentration (5 mmol L<sup>-1</sup>) and selectivity (4%).

During the first 10 h reaction time, adipic acid monomethyl ester was identified at concentration values extremely low, with a sharp increase between 10 and 14 h reaction time. After that, it seems to remain constant as well as HHH concentration.

The products obtained with catalyst RuSn/Al-PILC are presented in Fig. 11. As verified in Table 2, the presence of tin causes considerable changes in the behavior of the system. This catalyst produced two new compounds that were not identified in other media reaction: methyl caproate and γ-caprolactone. Methyl caproate (MC) presents a concentration increasing throughout the 15 h reaction time analyzed. Similarly to the behavior observed with methyl caproate and to a lesser extent with ε-caprolactone, γ-caprolactone concentration also increases throughout the reaction period. The behavior of hexane, MME and hexanoic acid follow a similar pattern: their concentration increase until the third hour and there

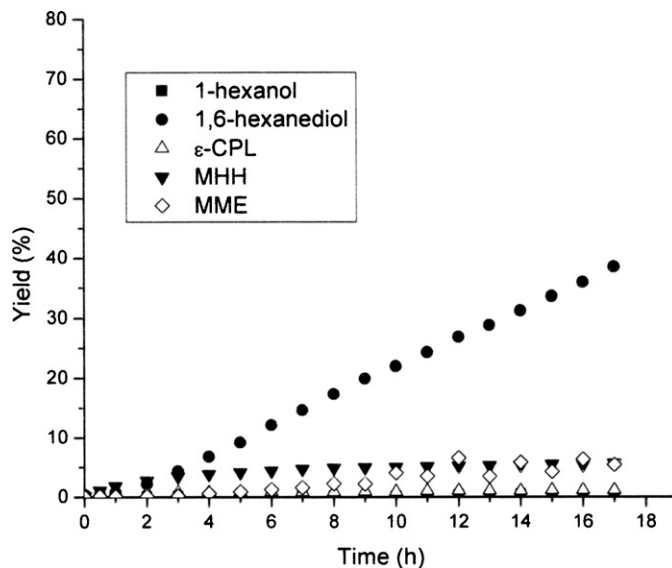


Fig. 9. Yield of dimethyl adipate hydrogenation by RuSn/SiO<sub>2</sub> catalyst.

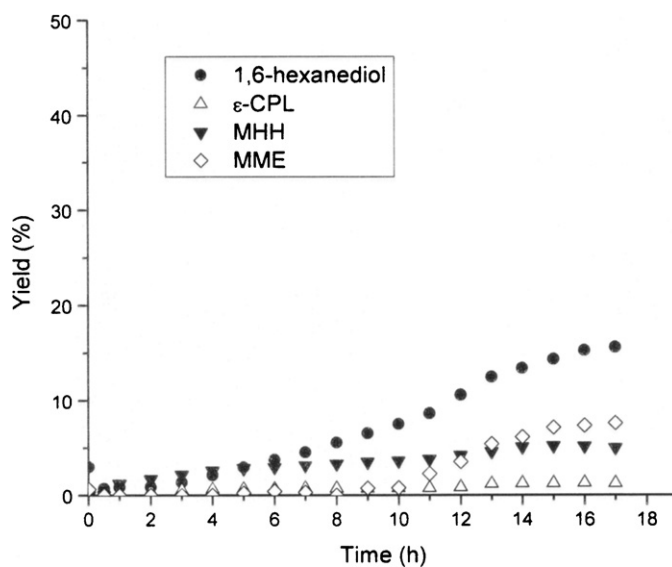


Fig. 10. Yield of dimethyl adipate hydrogenation by RuSn/Nb<sub>2</sub>O<sub>5</sub> catalyst.

is a subsequent consumption, indicating that these products are undergoing further conversions in the reaction media.

Even though this catalyst has presented a similar reduction profile of the bimetallic silica, niobia and anatase titania, in this reaction medium the formation of 1,6-hexanediol was identified in small concentrations, indicating an intrinsic role of the support.

The RuSn/Al-PILC catalyst was also modified with barium. The results to RuSn/Al-PILC-Ba catalyst are shown in Fig. 12.

The presence of barium slightly reduces the activity, but deeply changes the selectivity of the system. We observed similar behavior to the non-modified catalyst, but a significant reduction in the

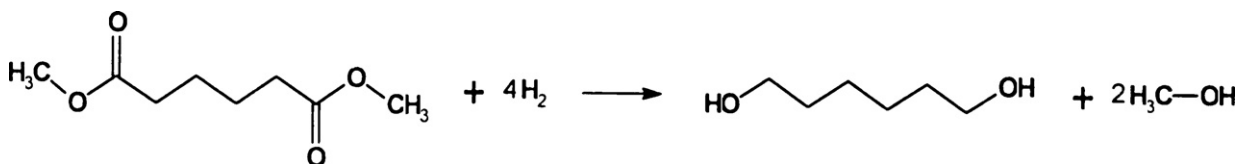


Fig. 8. 1,6-hexanediol formation from dimethyl adipate hydrogenation.

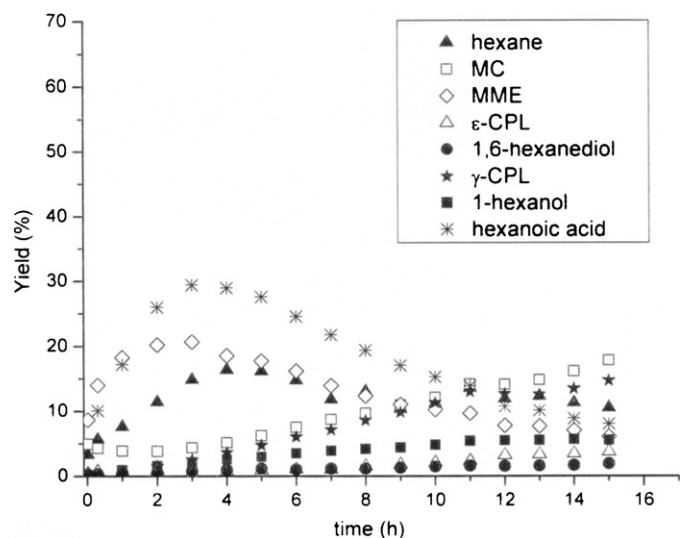


Fig. 11. Yield of dimethyl adipate hydrogenation by RuSn/Al-PILC catalyst.

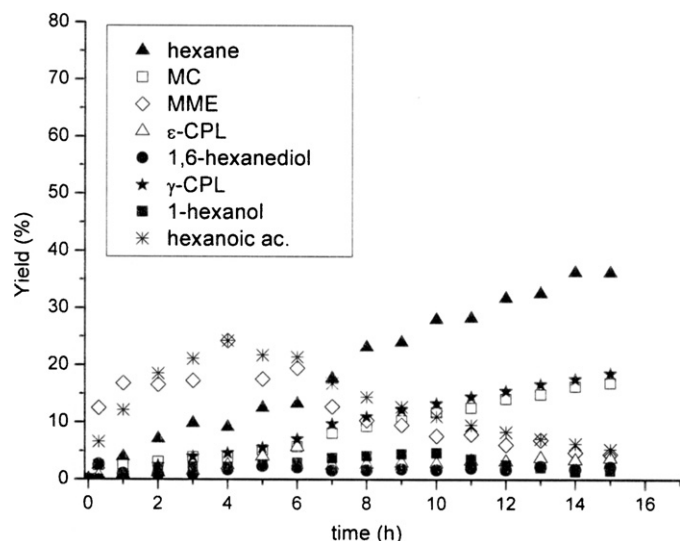


Fig. 12. Yield of dimethyl adipate hydrogenation by RuSn/Al-PILC-Ba catalyst.

concentration of hexanoic acid and substantial increase in the hexane concentration. We can assume that the presence of barium is favoring the hydrogenation of hexanoic acid to the corresponding alkane.

According to results showed in previous work [2] the deposition of barium on the RuSn/Al-PILC catalyst causes important modifications in the catalyst. Ruthenium active area diminishes, since barium cations partially recover ruthenium particles. Moreover, Lewis acid sites are practically eliminated, which is related to the neutralization of aluminol groups [29,30]. It is suggested that the low selectivity presented by the use of pillared clays is caused by an abundant acid sites (both Bronsted and Lewis) that catalyze isomerization and cracking reactions. The reduction of acidity with barium leads the system to be more selective to the main products, reducing the concentration of “other” products. However the catalysts supported over pillared clays did not show high diol concentration, while these systems allow the formation of valuable products as lactones and methyl caproate.

#### 4. Conclusions

Strong metal–support interaction (SMSI) established important differences in both catalytic activity and selectivity of hydrogenation

reaction. The results allow us to conclude that the support may alter the metal–promoter interaction (besides the metal–support interaction) and their reduction profiles, consequently changing the behavior of the catalysts.

The use of pillared clays lead to high conversions for both monometallic and bimetallic system, typically higher than 95%, which may be attributed to a support activity. The reduction of the catalyst acidity through modification with barium deeply modified the formation of undesirable products as well as the distribution of the products.

In the oxides supported catalysts, it was evidenced distinct conversions and products formation, indicating the main role played by tin on the activation of ester carbonyl group. The presence of reducible support species also showed a promoting effect over selectivity, especially to 1,6-hexanediol, suggesting a combined effect between support and tin promoter. Active sites obtained to RuSn/TiO<sub>2</sub>-A, RuSn/SiO<sub>2</sub> and RuSn/Nb<sub>2</sub>O<sub>5</sub> catalysts were suitable for the hydrogenation of the ester group of dimethyl adipate leading to a selective conversion to 1,6-hexanediol.

#### Acknowledgements

The authors thank FAPESP (2006/04142-0 and 2009/07109-2), CAPES and CNPq for their financial support, UNICAMP, UFLA and PUC-Campinas for their support on the development of the studies.

#### References

- [1] M. Toba, S.I. Tanka, S.I. Niwa, F. Mizukami, S. Koppány, L. Guezi, K.Y. Cheah, T.S. Tang, *Appl. Catal.* 189 (1999) 243–250.
- [2] F.C.A. Figueiredo, E. Jordão, R. Landers, W.A. Carvalho, *Appl. Catal. A: Gen.* 371 (2009) 131–141.
- [3] V. Poncet, *Appl. Catal. A: Gen.* 149 (1997) 27–48.
- [4] B. Chen, U. Dingerdissen, J.G.E. Krauter, H.G.J. Lansik Rotgerink, K. Mobus, D.J. Ostgard, P. Panster, T.H. Riermeier, S. Seebald, T. Tacke, H. Trauthwein, *Appl. Catal. A* 280 (2005) 17–46.
- [5] F.C.A. Figueiredo, E. Jordão, W.A. Carvalho, *Catal. Today* 223 (2005) 107–108.
- [6] F.C.A. Figueiredo, E. Jordão, W.A. Carvalho, *Appl. Catal. A* 351 (2008) 259–269.
- [7] S.M. Santos, A.M. Silva, E. Jordão, M.A. Fraga, *Catal. Commun.* 5 (2004) 377–381.
- [8] S.J. Tauster, S.C. Fung, R.L.J. Garten, *Am. Chem. Soc.* 100 (1978) 170–175.
- [9] T. Uchijima, *Catal. Today* 28 (1996) 105–117.
- [10] S.M. Dal Bosco, R.S. Jimenez, C. Vignado, J. Fontana, B. Geraldo, F.C.A. Figueiredo, D. Mandelli, W.A. Carvalho, *Adsorption* 12 (2006) 133–146.
- [11] A.M. Silva, O.A.A. Santos, E.M. Baggio-Saitovitch, E. Jordão, M.A. Fraga, *J. Mol. Catal. A* 253 (2006) 62–70.
- [12] A.M. Silva, M.A. Morales, E.M. Baggio-Saitovitch, E. Jordão, M.A. Fraga, *Appl. Catal. A: Gen.* 353 (2009) 101–106.
- [13] S.M. Santos, A.M. Silva, E. Jordão, M.A. Fraga, *Catal. Today* 107–108 (2005) 250–258.
- [14] P. Reyes, M.E. Kong, G. Pecchi, I. Concha, M.L. Granados, J.L.G. Fierro, *Catal. Lett.* 46 (1997) 71–75.
- [15] L. Jinxiang, Y. Lixin, G. Shiuying, H. Lijuan, T. Renyuan, D. Dongbai, *Thermochim. Acta* 123 (1988) 121–133.
- [16] G.R. Gallaher, J.G. Goodwin Jr., L. Guzzi, *Appl. Catal. A: Gen.* 73 (1991) 1–15.
- [17] J. Fan, X. Wu, L. Yang, D. Weng, *Catal. Today* 126 (2007) 303–312.
- [18] I.Y. Ahn, W.J. Kim, S.H. Moon, *Appl. Catal. A: Gen.* 308 (2006) 75–81.
- [19] A.M. Silva, O.A.A. Santos, M.J. Mendes, E. Jordão, M.A. Fraga, *Appl. Catal. A: Gen.* 241 (2003) 155–165.
- [20] J.N. Coupé, E. Jordão, M.A. Fraga, M.J. Mendes, *Appl. Catal. A* 199 (2000) 45–51.
- [21] Y. Li, Y. Fan, H. Yang, B. Xu, L. Feng, M. Yang, Y. Chen, *Chem. Phys. Lett.* 372 (2003) 160–165.
- [22] T.M. Salama, H. Hattori, H. Kita, K. Ebitani, T. Tanaka, *J. Chem. Soc. Faraday Trans.* 89 (1993) 2067–2075.
- [23] K. Tahara, E. Nagahara, S. Itoi, S. Nishiyama, S. Tsuruya, M. Masai, *Appl. Catal. A: Gen.* 154 (1997) 75–86.
- [24] P. Mäki-Arvela, J. Hájek, T. Salmi, D.Yu. Murzin, *Appl. Catal. A: Gen.* 292 (2005) 1–49.
- [25] P. Reyes, M.C. Aguirre, J.L.G. Fierro, G. Santori, O. Ferretti, *J. Mol. Catal. A: Chem.* 184 (2002) 431–441.
- [26] U.K. Singh, M.A. Vannice, *Appl. Catal. A: Gen.* 213 (2001) 1–24.
- [27] R. Chen, Y. Du, W. Xing, N. Xu, Chin. J. Chem. Eng. 5 (2006) 665–669.
- [28] M. English, V.S. Ranade, J.A. Lercher, *J. Mol. Catal. A: Chem.* 121 (1997) 69–80.
- [29] V. Labalme, N. Benhamou, N. Guilhaume, E. Garbowski, M. Primet, *Appl. Catal. A* 133 (1995) 351–366.
- [30] V. Labalme, B. Béguin, F. Gailard, M. Primet, *Appl. Catal. A* 192 (2000) 307–316.